Inorganic Chemistry
Article

Inorg. Chem. **2010**, *49*, 8389–8400 **8389**
DOI: 10.1021/ic101030h

Porphyrin−Fullerene, C_{60}, Cocrystallates: Influence of C_{60} on the Porphyrin Ring Conformation

P. Bhyrappa* and K. Karunanithi

Department of Chemistry, Indian Institute of Technology Madras Chennai 600 036, India

Received May 21, 2010

To examine the influence of fullerene on the macrocyclic ring conformation, crystal structures of a series of cocrystals of 2,3,5,10,12,13,15,20-octaphenylporphyrin, M(TPP)$(Ph)_4$ (M = 2H, Co(II), Cu(II)), and 2,312,13-tetramethyl-5,7,8,10,15,17,18,20-octaphenyl-porphinato copper(II), CuTPP$(Ph)_4(CH_3)_4$, derivatives with fullerene, C_{60}, were elucidated. Furthermore, crystal structures of the parent porphyrins, M(TPP)$(Ph)_4$ (M = Co(II), Cu(II)) complexes, were also determined. All the cocrystals revealed one-to-one stoichiometry between the porphyrin and C_{60} and were free of lattice solvates. Porphyrin rings in M(TPP)$(Ph)_4 \cdot C_{60}$ cocrystals revealed significant distortion with the root-mean-square (rms) value as high as 0.265(2) Å which is the average deviation of the 24 atoms core from the least-squares plane. Crystal structures of the parent M(TPP)$(Ph)_4$ (M = Co(II), Cu(II)) complexes indicated near planarity of the 24-atom core with the root-mean-square deviation value of 0.016(2) Å. Molecular packing in the M(TPP)$(Ph)_4 \cdot C_{60}$ cocrystals showed essentially one-dimensional chains interconnected by weak interporphyrin and porphyrin−fullerene close contacts. The $N_{porphyrin} \cdots C(C_{60})$ shortest distances between the H_2(TPP)$(Ph)_4$ (M = 2H, Co(II), Cu(II)) and fullerene in the cocrystals are 3.031(5) Å, 3.062(4) Å, and 3.059(3) Å, respectively. Similarly, close contact M$\cdots$C distances in the M(TPP)$(Ph)_4 \cdot C_{60}$ (M = Co(II), Cu(II)) are 2.761(6) Å and 2.886(3) Å, respectively. In the Cu(TPP)$(Ph)_4(CH_3)_4 \cdot C_{60}$ cocrystal, the shift of macrocyclic ring toward planarity was evidenced from the rms value of 0.236(2) Å relative to that observed in CuTPP$(Ph)_4(CH_3)_4 \cdot CHCl_3$ (0.391(2) Å). The distortion of the macrocyclic ring in M(TPP)$(Ph)_4 \cdot C_{60}$ complexes was examined by normal-coordinate-structure decomposition (NSD) analyses. Their out-of-plane displacement of the core atoms revealed predominant contribution being *saddle* (∼95−96%) and gentle *domed* distortions (3−4%). In the case of M(TPP)$(Ph)_4(CH_3)_4 \cdot C_{60}$ cocrystal, it showed mainly *saddled* (∼83%), minimal *ruffled* (8%) and *domed* (8%) distortions of the macrocyclic ring. In-plane displacement on the 24-atom core of the porphyrin in these cocrystallates features generally a varying degree of N-*str* (B_{1g}) and *bre* (A_{1g}) distortions.

Introduction

Since the discovery of Buckminsterfullerene, C_{60},[1a] there has been numerous reports on the [60] fullerene based materials because of their unique electronic and physicochemical properties.[1b,c] Fullerenes as three-dimensional electron acceptors with various electron donor molecules have been reported in the literature.[2−9] Porphyrins in association with fullerenes are of considerable attention owing to their potential use in material applications.[10] The large extended π-system of the flat porphyrin form weak donor−acceptor type of complexes with the electron deficient fullerene.[11,12] Monomeric porphyrins such as octaethylporphyrin,[13] tetraarylporphyrin,[14] tetraazaporphyrin[15] and their metal complexes have been examined as lattice host for the complexation

*To whom correspondence should be addressed. E-mail: byra@iitm.ac.in.

(1) (a) Kroto, H. W.; Heath, J. R.; O'Brien, S. C.; Curl, R. F.; Smalley, R. E. *Nature* **1985**, *318*, 162. (b) Sariciftci, N. S.; Heeger, A. J. *Handbook of Organic Conductive Molecules and Polymers*; Nalwa, H. S., Ed.; John Wiley and Sons Ltd.: New York, 1997; Vol. *1*, pp 414−457. (c) Kawase, T.; Kurata, H. *Chem. Rev.* **2006**, *106*, 5250 and references therein.
(2) Stephens, P. W.; Cox, D.; Lauher, J. W.; Mihaly, L.; Wiley, J. B.; Allemand, P.-M.; Hirsh, A.; Holczer, K.; Li, Q.; Tompson, J. D.; Wudl, F. *Nature* (*London*) **1992**, *355*, 331.
(3) Wan, W. C.; Liu, X.; Sweeney, G. M.; Broderick, W. E. *J. Am. Chem. Soc.* **1995**, *117*, 9580.
(4) Konarev, D. V.; Lyubovskaya, R. N. *Russ. Chem. Rev.* **1999**, *68*(1), 19.
(5) Konarev, D. V.; Lyubovskaya, R. N.; Drichko, N. V.; Yudanova, E. I.; Shul'ga, Yu. M.; Litvinov, A. L.; Semkin, V. N.; Tarasov, B. P. *J. Mater. Chem.* **2000**, 803.
(6) Izuoka, A.; Tachikawa, T.; Sugawara, T.; Suzuki, Y.; Konno, M.; Saito, Y.; Shinohara, H. *J. Chem. Soc., Chem. Commun.* **1992**, 1472.
(7) Crane, J. D.; Hitchcock, P. B.; Kroto, H. W.; Taylor, R.; Walton, R. M. *J. Chem. Soc., Chem. Commun.* **1992**, 1764.
(8) Saito, G.; Teramoto, T.; Otsuka, A.; Sugita, Y.; Ban, T.; Kusunoki, M.; Sakaguchi, K. *Synth. Met.* **1994**, *64*, 359.
(9) Konarev, D. V.; Zubavichus, Y. V.; Slovokhotov, Yu. L.; Shul'ga, Yu. M.; Semkin, V. N.; Drichko, N. V.; Lyubovskaya, R. N. *Synth. Met.* **1998**, *92*, 1.
(10) Roncali, J. *Acc. Chem. Res.* **2009**, *42*, 1719 and references cited therein.
(11) Boyd, P. D. W.; Reed, C. A. *Acc. Chem. Soc.* **2005**, *38*, 235.
(12) (a) Balch, A. L.; Olmstead, M. M. *Coord. Chem. Rev.* **1999**, *185*−*186*, 601. (b) Ishii, T.; Aizawa, N.; Kanehama, R.; Yamashita, M.; Sugiura, K.-I.; Miyasaka, H. *Coord. Chem. Rev.* **2002**, *226*, 113.

Published on Web 08/19/2010

of fullerenes. The theoretical calculations on porphyrin−fullerene interaction energies involve the electrostatic attractive forces that are offset by the Pauli repulsive interactions[16a,d] and/or London dispersion forces.[16b−d] Porphyrins and metalloporphyrins are potentially attractive molecular candidates because of their ease of synthesis, facile functionalization, extended π-system, and capable of incorporating a wide range of metal ions with tunable stereochemistry of the macrocycle.[17]

Porphyrin−fullerene conjugates have been studied extensively as model compounds for energy and electron transfer reactions.[18] The incorporation of fullerenes into the porphyrin network led to the formation of donor−acceptor complexes via weak noncovalent interactions.[19] Such a weak porphyrin−fullerene interaction was exploited in the separation of fullerenes by silica gel appended porphyrins.[20] Moreover, with the increase in number of porphyrin units in the ensembles as in dimeric,[21] trimeric porphyrin,[22] tetramer,[23] pentaphyrin box,[24] and hexamer[25] have been employed as molecular hosts for complexation with the fullerenes. The cofacial bisporphyrins are capable of incorporating fullerenes into their cavities. Such cyclic porphyrin dimers have been employed in selective extraction of higher fullerenes.[26]

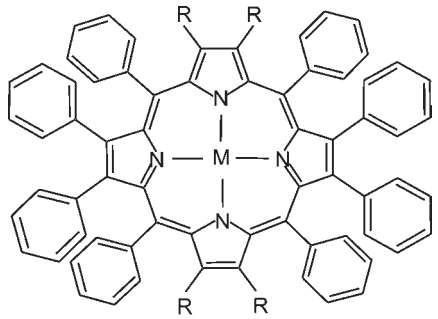

Figure 1. Molecular structures of porphyrins (M(TPP)$(Ph)_4$) and Cu(TPP)$(Ph)_4(CH_3)_4$ employed for cocrystallization with C_{60}.

The porphyrin−fullerene cocrystallates thus far reported, in general, have planar geometry of the macrocycle. The increase in peripheral substituents induce nonplanar porphyrin ring conformation/or flexible porphyrin core, and such porphyrins have been largely unexamined for the complexation with fullerenes. Crystal structures of β-tetra(phenyl/methyl/bromo) substiuted H_2(TPP)s[27] revealed an increase in average N_4H_2 core expansion[28a] relative to H_2(TPP),[29] and more flexibility of the ring conformation was noticed for β-octasubstituted H_2(TPP)s.[30,31] Complexation some of these β-pyrrole functionalized MTPPs (Figure 1) with C_{60} has been undertaken to elucidate the role of spherical C_{60} on the porphyrin ring conformational flexibility and the supramolecular intermolecular interactions between them. The present article reports about the M(TPP)$(Ph)_4\cdot C_{60}$ (M = 2H, Cu(II), Co(II))[32] and

(13) (a) Olmstead, M. M.; Costa, D. A.; Maitra, K.; Noll, B. C.; Phillips, S. L.; Van Calcar, P. M.; Balch, A. L. *J. Am. Chem. Soc.* **1999**, *121*, 7090. (b) Ishii, T.; Aizawa, N.; Yamashita, M.; Matsuzaka, H.; Kodama, T.; Kikuchi, K.; Ikemoto, I.; Iwasa, Y. *J. Chem. Soc., Dalton Trans.* **2000**, 4407. (c) Konarev, D. V.; Khasanov, S. S.; Saito, G.; Lyubovskaya, R. N. *Cryst. Growth Des.* **2009**, *9*, 1170.

(14) (a) Boyd, P. D. W.; Hodgson, M. C.; Rickard, C. E. F.; Oliver, A. G.; Chaker, L.; Brothers, P. J.; Bolskar, R. D.; Tham, F. S.; Reed, C. A. *J. Am. Chem. Soc.* **1999**, *121*, 10487. (b) Konarev, D. V.; Neretin, I. S.; Slovokhotov, Yu. L.; Yudanova, E. I.; Drichko, N. V.; Shul'ga, Yu. M.; Tarasov, B. P.; Gumanov, L. L.; Batsanov, A. S.; Howard, J. A. K.; Lyubovskaya, R. N. *Chem.—Eur. J.* **2001**, *7*, 2605. (c) Konarev, D. V.; Kovalevsky, A. Y.; Li, X.; Neretin, I. S.; Litvinov, A. L.; Drichko, N. V.; Slovokhotov, Y. L.; Coppens, P.; Lyubovskaya, R. N. *Inorg. Chem.* **2002**, *41*, 3638. (d) Konarev, D. V.; Khasanov, S. S.; Saito, G.; Lyubovskaya, R. N.; Yoshida, Y.; Otsuka, A. *Chem.—Eur. J.* **2003**, *9*, 3837. (e) Hosseini, A.; Hodgson, M. C.; Tham, F. S.; Reed, C. A.; Boyd, P. D. W. *Cryst. Growth Des.* **2006**, *6*, 397. (f) Olmstead, M. M.; Nurco, D. J. *Cryst. Growth Des.* **2006**, *6*, 109.

(15) (a) Eichhorn, D. M.; Yang, S.; Jarrell, W.; Baumann, T. F.; Beall, L. S.; White, A. J. P.; Williams, D. J.; Barrett, A. G. M.; Hoffman, B. M. *J. Chem. Soc., Chem. Commun.* **1995**, 1703. (b) Hochmuth, D. H.; Michel, S. L. J.; White, A. J. P.; Williams, D. J.; Barrett, A. G. M.; Hoffman, B. M. *Eur. J. Inorg. Chem.* **2000**, 593.

(16) (a) Wang, Y.-B.; Zhenyang, L. *J. Am. Chem. Soc.* **2003**, *125*, 6072. (b) Jung, Y.; Head-Gordon, M. *Phys. Chem. Chem. Phys.* **2006**, *8*, 2631. (c) Liao, M.-S.; Watts, J. D.; Huang, M.-J. *J. Phys. Chem. B* **2007**, *111*, 4374. (d) Huheey, J. E., Keiter, E. A., Keiter, R. L., Eds. Instantaneous dipole-induced dipole interactions are sometimes refereed to as London dispersion forces or van der Waals forces. *Inorganic Chemistry: Principles of Structure and Reactivity*, 4th ed.; Addison-Wesley Publishing Co.: New York, 1993.

(17) Kadish, K. M.; Smith, K. M.; Guilard, R. *The Porphyrin Handbook*; Academic Press: San Diego, 2000, Vols. *1*−*10*, and references cited therein.

(18) (a) Guldi, D. M. *Chem. Soc. Rev.* **2002**, *31*, 22. (b) Chitta, R.; D'Souza, F. *J. Mater. Chem.* **2008**, *18*, 1440, and references therein.

(19) (a) Sun, D.; Tham, F. S.; Reed, C. A.; Boyd, P. D. W. *Proc. Natl. Acad. Sci. U.S.A.* **2002**, *99*, 5088. (b) Taylor, S. K.; Jameson, G. B.; Boyd, P. D. W. *Supramol. Chem.* **2005**, *17*, 543.

(20) Xiao, J.; Savina, M. R.; Martin, G. B.; Francis, A. H.; Meyerhoff, M. E. *J. Am. Chem. Soc.* **1994**, *116*, 9341.

(21) (a) Sun, D.; Tham, F. S.; Reed, C. A.; Chaker, L.; Burgess, M.; Boyd, P. D. W. *J. Am. Chem. Soc.* **2000**, *122*, 10704. (b) Tashiro, K.; Aida, T.; Zheng, J.-Y.; Kinbara, K.; Saigo, K.; Sakamoto, S.; Yamaguchi, K. A. *J. Am. Chem. Soc.* **1999**, *121*, 9477. (c) Zheng, J.-Y.; Tashiro, K.; Hirabayashi, Y.; Kinbara, K.; Saigo, K.; Aida, T.; Sakamoto, S.; Yamaguchi, K. *Angew. Chem., Int. Ed.* **2001**, *40*, 1858. (d) Ayabe, M.; Ikeda, A.; Shinkai, S.; Sakamoto, S.; Yamaguchi, K. A. *Chem. Commun.* **2002**, *10*, 1032. (e) Dudic, M.; Lhotak, P.; Stibor, I.; Petrickova, H.; Lang, K. *New. J. Chem.* **2004**, *28*, 85. (f) Dannhuser, J.; Donaubauer, W.; Hampel, F.; Reiher, M.; Guennic, B. L.; Corzilius, B.; Dinse, K.-P.; Hirsch, A. *Angew. Chem. Int. Ed.* **2006**, *45*, 3368.

(22) Tong, L. H.; Wietor, J.-L.; Clegg, W.; Raithby, P. R.; Pascu, S. I.; Sanders, J. K. M. *Chem.—Eur. J.* **2008**, *14*, 3035.

(23) Kubo, Y.; Sugasaki, A.; Ikeda, M.; Sugiyasu, K.; Sonoda, K.; Ikeda, A.; Takeuchi, M.; Shinkai, S. *Org. Lett.* **2002**, *4*, 925.

(24) Kimura, M.; Saito, Y.; Ohta, K.; Hanabusa, K.; Shirai, H.; Kobayashi, N. *J. Am. Chem. Soc.* **2002**, *124*, 5274.

(25) Ayabe, M.; Ikeda, A.; Kubo, Y.; Takeuchi, M.; Shinkai, S. A. *Angew. Chem., Int. Ed.* **2002**, *41*, 2790.

(26) Shoji, Y.; Tashiro, K.; Aida, T. *J. Am. Chem. Soc.* **2004**, *126*, 6570.

(27) (a) Chan, K. S.; Zhou, X.; Lou, B.-S.; Mak, T. C. W. *J. Chem. Soc., Chem. Commun.* **1994**, 271. (b) Zou, J.-H.; Xu, Z. I. M.; You, X.-Z. *Acta Crystallogr.* **1995**, *C51*, 760. (c) Bhyrappa, P.; Karunanithi, K.; Varghese, B. *Acta Crystallogr.* **2007**, *E63*, o4755.

(28) (a) Scheidt, W. R. In *The Porphyrin Handbook*; Kadish, K. M., Smith, K. M., Guilard, R., Eds.; Academic Press: New York, 2000; Vol. *3*, p 49. (b) Scheidt, W. R.; Lee, Y. J. *Struct. Bonding* (*Berlin*) **1987**, *64*, 1.

(29) Silvers, S. J.; Tulinsky, A. *J. Am. Chem. Soc.* **1967**, *89*, 3331.

(30) Senge, M. O. In *The Porphyrin Handbook*; Kadish, K. M., Smith, K. M., Guilard, R., Eds.Academic Press: New York, 2000; Vol. *1*, p 239, and references therein.

(31) (a) Shelnutt, J. A.; Song, X.-Z.; Ma, J.-G.; Jia, S.-L.; Jentzen, W.; Medforth, C. J. *Chem. Soc. Rev.* **1998**, *27*, 31, and references therein. (b) Renner, M. W.; Furenlid, L. R.; Barkigia, K. M.; Forman, A.; Shim, H.-K.; Smith, K. M.; Fajer, J. *J. Am. Chem. Soc.* **1991**, *113*, 6891. (c) Furenlid, L. R.; Renner, M. W.; Fajer, J. *J. Am. Chem. Soc.* **1990**, *112*, 8987. (d) Barkigia, K. M.; Renner, M. W.; Furenlid, L. R.; Medforth, C. J.; Smith, K. M.; Fajer, J. *J. Am. Chem. Soc.* **1993**, *115*, 3627. (e) Sparks, L. D.; Medforth, C. J.; Park, M.-S.; Chamberlain, J. R.; Ondrias, M. R.; Senge, M. O.; Smith, K. M.; Shelnutt, J. A. *J. Am. Chem. Soc.* **1993**, *115*, 581. (f) Shelnutt, J. A.; Medforth, C. J.; Berber, M. D.; Barkigia, K. M.; Smith, K. M. *J. Am. Chem. Soc.* **1991**, *113*, 4077. (g) Senge, M. O.; Medforth, C. J.; Sparks, L. D.; Shelnutt, J. A.; Smith, K. M. *Inorg. Chem.* **1993**, *32*, 1716. (h) Renner, M. W.; Barkigia, K. M.; Zhang, Y.; Medforth, C. J.; Smith, K. M.; Fajer *J. Am. Chem. Soc.* **1994**, *116*, 8582. (i) Terazono, Y.; Patrick, B. O.; Dolphin, D. *Inorg. Chem.* **2002**, *41*, 6703.

(32) (a) Bhyrappa, P.; Sankur, M.; Varghese, B. *Inorg. Chem.* **2006**, *45*, 4136. (b) Bhyrappa, P.; Karunanithi, K.; Varghese, B. *Acta Crystallogr.* **2008**, *E64*, m330.

Table 1. Crystal Structure Data of Porphyrin−C_{60} Cocrystallates and Their Parent Porphyrin Structures

	$H_2(TPP)(Ph)_4\cdot C_{60}$	$Co(TPP)(Ph)_4\cdot C_{60}$	$Cu(TPP)(Ph)_4\cdot C_{60}$	$Cu(TPP)(Ph)_4(CH_3)_4\cdot C_{60}$	$Co(TPP)(Ph)_4$	$Cu(TPP)(Ph)_4$
empirical formula	$C_{512}H_{184}N_{16}$	$C_{512}H_{176}N_{16}$	$C_{512}H_{176}N_{16}$	$C_{528}H_{208}N_{16}Cu_4$	$C_{136}H_{88}N_8Cu_2$	$C_{136}H_{88}N_8Cu_2$
fw	1639.69	1696.60	1701.22	1757.33	976.0	980.61
color	black	black	black	black	brown	purple
crystal system	orthorhombic	orthorhombic	orthorhombic	monoclinic	monoclinic	monoclinic
space group	*Cmcm*	*Cmcm*	*Cmcm*	*C*2/*c*	$P2_1/c$	$P2_1/c$
a, Å	28.3412(13)	28.2701(20)	28.2090(15)	28.8907(6)	7.4849(3)	7.5140(2)
b, Å	12.3443(5)	12.2664(8)	12.5098(6)	12.8854(2)	13.2326(5)	13.2397(4)
c, Å	22.1155(9)	22.0499(14)	22.0235(8)	23.6560(5)	24.4198(10)	24.4967(8)
α (°)	90	90	90	90	90	90
β (°)	90	90	90	115.758(1)	92.799(2)	92.630(2)
γ (°)	90	90	90	90	90	90
vol (Å^3)	7737.2(6)	7646.3(9)	7771.9(6)	7931.4(3)	2415.77(17)	2434.44(13)
Z	4	4	4	4	2	2
D_{calcd}(mg/m^3)	1.408	1.474	1.454	1.472	1.342	1.338
wavelength (*λ*), Å	0.71073	0.71073	0.71073	0.71073	0.71073	0.71073
T (K)	173(2)	173(2)	173(2)	173(2)	173(2)	173(2)
no. of unique reflections	3630	3409	3590	6966	4232	5938
no. of parameters refined	307	312	311	620	331	331
GOF on F^2	1.057	1.261	1.138	1.156	1.031	1.011
R_1[a]	0.0475	0.0673	0.0357	0.0372	0.0343	0.0381
wR_2[b]	0.1339	0.1856	0.1044	0.1062	0.0782	0.0878

[a] $R_1 = \sum||F_o| - |F_c||/\sum|F_o|$; $I_o > 2\sigma(I_o)$. [b] $wR_2 = [\sum w(F_o^2 - F_c^2)^2/\sum w(F_o^2)^2]^{1/2}$.

$Cu(TPP)(Ph)_4(CH_3)_4\cdot C_{60}$ cocrystallates, and the macrocycle in the former cocrystallates revealed nonplanarity while the porphyrin ring is less distorted in the latter case. Further, normal-coordinate-structure decomposition analysis of the macrocycles in these cocrystallates is also reported.

Experimental Section

Materials. 2,3,5,10,12,13,15,20-Octaphenylporphyrin, $H_2(TPP)(Ph)_4$, and its (M = Cu(II), Co(II)) complexes and highly substituted 2,3,12,13-tetramethyl-5,7,8,10,15,17,18,20-octaphenylporphinato copper(II) were prepared (Figure 1) using literature methods.[32] Fullerene, C_{60}, 1,1,2,2-tetrachloroethane (TCE), and *n*-hexane purchased from Sigma-Aldrich (India) were of analytical grade and used as received.

Instrumentation. Single-crystal X-ray structure data collections were performed on a Bruker AXS Kappa Apex II CCD diffractometer with graphite monochromated Mo Kα radiation equipped with liquid nitrogen cryostat.

Crystal Structures. Crystals of $M(TPP)(Ph)_4\cdot C_{60}$ (M = 2H, Co(II), Cu(II)) were grown by diffusing *n*-hexane vapor to the saturated solution containing equimolar concentrations of porphyrin and fullerene in TCE over a period of 7 days. Similarly, $Cu(TPP)(Ph)_4(CH_3)_4\cdot C_{60}$ cocrystals were grown by diffusing *n*-hexane to the porphyrin/C_{60} in TCE over a period of 3 days.

The dark brown platelike/needle shaped crystals were coated with inert oil, mounted on a glass capillary using quick fix glue, and transferred to the cold nitrogen gas stream of the diffractometer, and crystal data were collected at 173 K. The reflections with $I > 2\sigma(I)$ were used for structure solution and refinement. The SIR92[33,34] (WINGX32) program was employed for solving the structure by direct methods. Successive Fourier synthesis was employed to complete the structures after full-matrix least-squares refinement on $|F|^2$ using the SHELXL97 software. Fourier syntheses led to the location of all of the nonhydrogen atoms. The criterion of $F^2 > 2\sigma(F^2)$ was employed for calculating *R*1. Nonhydrogen atoms were refined with anisotropic thermal parameters. Hydrogen atoms of the porphyrin structures were geometrically relocated at chemically meaningful positions and given riding model refinement. In the case of $H_2(TPP)(Ph)_4\cdot C_{60}$ complex, the imino hydrogens show disorder on all the four pyrrole nitrogens and are fixed using riding model refinement. Intermolecular short contacts were calculated from Platon,[35] and molecular packing motifs were drawn using Mercury 2.2 software.[36] ORTEP diagrams were generated using ORTEP-3 for windows program.[37]

Results and Discussion

$M(TPP)(Ph)_4\cdot C_{60}$ (M = 2H, Co(II), Cu(II)) cocrystallates were grown from the same solvent system to elucidate the influence of C_{60} on the stereochemistry of the porphyrin ring. Crystal structure data of the cocrystallates are listed in Table 1. All the $M(TPP)(Ph)_4\cdot C_{60}$ cocrystals are isomorphous and crystallized in orthorhombic space group, *Cmcm*, with $Z = 4$. The asymmetric unit contains one-quarter of each porphyrin and C_{60}, and both have crystallographic *mm*2 symmetry.

The bond lengths and geometrical parameters along the transannular pyrrole directions are listed in Table 2. For comparison, the crystal structure of $M(TPP)(Ph)_4$ (M = Co(II), Cu(II)) complexes were examined and the data is also incorporated in Table 2. Both the porphyrin complexes, $M(TPP(Ph)_4$ (M = Co(II), Cu(II)), crystallize in isomorphous monoclinic space group $P2_1/c$ as in the $H_2(TPP)(Ph)_4$ structure.[27a] These porphyrin/C_{60} complexes crystallize in 1:1 stoichiometry and are free of lattice solvates. The majority of the reported porphyrin/C_{60} crystallates bear a varying degree of lattice solvates.[11−14] As reported earlier, $H_2(TPP)$ and its metal complexes are known to form clathrates by incorporating a wide range of lattice solvates.[38]

A representative ORTEP diagram of $H_2(TPP)(Ph)_4\cdot C_{60}$ is shown in Figure 2. In general, the mean bond lengths of the porphyrin ring in the $M(TPP)(Ph)_4\cdot C_{60}$ (M = 2H, Co(II), Cu(II)) cocrystallates are comparable to the parent $M(TPP)(Ph)_4$ (M = 2H, Co(II), Cu(II)) structures. The $M(TPP)(Ph)_4$ structures showed elongation of the core along the

(33) Sheldrick, G. M. *Acta Crystallogr., Sect. A* **2008**, *64*, 112.
(34) Altomare, A. G.; Cascarano, G.; Giacovazzo, C.; Gualardi, A. *J. Appl. Crystallogr.* **1993**, *26*, 343.
(35) Spek, A. L. *J. Appl. Crystallogr.* **2003**, *36*, 7.
(36) Bruno, I. J.; Cole, J. C.; Edgington, P. R.; Kessler, M.; Macrae, C. F.; McCabe, P.; Pearson, J.; Taylor, J. *Acta Crystallogr.* **2002**, *B58*, 389.
(37) Farrugia, L. J. *J. Appl. Crystallogr.* **1997**, *30*, 565.
(38) Byrn, M. P.; Curtis, C. J.; Hsiou, Y.; Khan, S. I.; Sawin, P. A.; Tendick, S. K.; Terzis, A.; Strouse, C. E. *J. Am. Chem. Soc.* **1993**, *115*, 9480.

Table 2. Selected Mean Bond Lengths and Geometrical Parameters of Porphyrin−C_{60} Cocrystallates and M(TPP)$(Ph)_4$ Structures

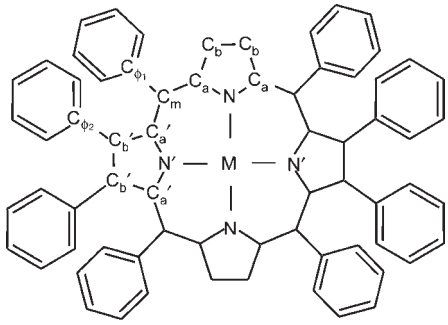

M = 2H, Co(II), Cu(II); M(TPP)$(Ph)_4$•C_{60}
M = 2H, Co(II), Cu(II); M(TPP)$(Ph)_4$

	$H_2(TPP)(Ph)_4 \cdot C_{60}$	$H_2(TPP)(Ph)_4$[a]	$Co(TPP)(Ph)_4 \cdot C_{60}$	$Co(TPP)(Ph)_4$	$Cu(TPP)(Ph)_4 \cdot C_{60}$	$Cu(TPP)(Ph)_4$
			Distance (Å)			
M−N			1.963(4)	1.947(2)	1.984(2)	1.959(1)
M−N′			2.001(4)	2.025(2)	2.037(2)	2.060(1)
$N-C_a$	1.372(2)	1.372(9)	1.377(4)	1.385(2)	1.373(2)	1.382(2)
$N'-C_a'$	1.372(2)	1.370(9)	1.387(4)	1.392(2)	1.377(2)	1.384(2)
C_a-C_b	1.438(3)	1.441(9)	1.433(5)	1.433(3)	1.439(3)	1.435(2)
$C_a'-C_b'$	1.454(3)	1.440(9)	1.446(5)	1.448(3)	1.455(2)	1.451(3)
C_b-C_b	1.349(4)	1.332(9)	1.343(8)	1.337(3)	1.347(4)	1.342(3)
$C_b'-C_b'$	1.364(4)	1.375(9)	1.359(7)	1.364(3)	1.361(4)	1.365(2)
C_a-C_m	1.401(3)	1.400(9)	1.390(5)	1.389(3)	1.439(3)	1.395(4)
$C_a'-C_m$	1.397(3)	1.410(9)	1.389(5)	1.392(3)	1.391(3)	1.396(2)
			Angle (°)			
$(N-M-N)_{adj}$			90.0(4)	90.0(1)	90.0(2)	90.0(6)
$(N-M-N)_{opp}$			177.6(2)	180.0(1)	177.9(1)	180.0(1)
$M-N-C_a$			127.0(2)	127.7(1)	126.4(1)	127.3(1)
$M-N'-C_a'$			127.1(2)	127.4(1)	126.4(1)	127.0(1)
$N-C_a-C_m$	126.9(2)	128.1(6)	126.3(3)	126.9(2)	126.5(2)	127.3(2)
$N'-C_a'-C_m'$	124.7(2)	124.0(6)	124.3(3)	124.4(2)	124.5(2)	124.2(2)
$N-C_a-C_b$	108.8(2)	110.1(6)	110.3(3)	110.4(2)	109.8(2)	109.9(2)
$N'-C_a'-C_b'$	107.9(2)	106.7(6)	110.2(3)	110.4(2)	109.6(2)	110.1(2)
C_a-N-C_a	107.5(2)	105.4(6)	105.1(3)	104.6(2)	106.1(2)	105.4(1)
$C_a'-N'-C_a'$	109.2(2)	110.9(6)	105.4(3)	105.2(2)	106.8(2)	105.9(1)
$C_b-C_a-C_m$	124.3(2)	121.8(7)	123.4(3)	122.7(2)	123.7(2)	122.8(2)
$C_b'-C_a'-C_m$	127.4(2)	129.2(6)	125.3(3)	125.2(2)	125.8(2)	125.7(2)
$C_a-C_m-C_a'$	125.6(2)	126.1(6)	123.3(3)	123.5(2)	124.1(1)	124.2(2)
$C_a-C_m-C_{\phi 1}$	115.0(2)	115.4(6)	115.9(3)	115.0(2)	115.5(2)	114.6(2)
$C_a'-C_m-C_{\phi 1}$	119.3(2)	118.6(6)	120.8(3)	121.5(2)	120.4(2)	121.2(2)
$C_a'-C_b'-C_{\phi 2}$	129.4(2)	129.4(6)	129.8(3)	130.4(2)	129.8(2)	130.5(2)
$N'-C_a'-C_m-C_a$	9.8(3)	1(1)	10.4(6)	1.5(3)	10.4(3)	1.3(3)
$C_b'-C_a'-C_m-C_{\phi 1}$	10.9(3)	1(1)	9.0(3)	1.4(3)	10.0(3)	1.5(3)
			Geometrical Parameters (Å)			
$N\cdots N^i$	4.044	3.924	3.925	3.894	3.968	3.918
$N'\cdots N'^i$	4.225	4.371	4.002	4.047	4.073	4.120
rms	0.250(2)	na[b]	0.253(3)	0.015(2)	0.265(2)	0.012(2)
ΔM[c] (±)			0.024(2)	0.022(2)	0.023(1)	0.015(2)
			Dihedral Angle (°)[d]			
meso-phenyl	66.6(1)	na[b]	68.8(1)	73.9(1)	68.7(1)	74.1(1)
β-phenyl	70.6(1)	na[b]	71.5(1)	71.0(1)	71.5(1)	71.3(1)

[a] Data ref 27a. [b] na, data not available. [c] ΔM, deviation of metal atom from the mean porphyrin ring plane. [d] Relative to porphyrin ring mean plane.

substituted pyrrole direction to prevent steric strain enforced by the *meso* and *β*-pyrrole phenyl groups, leading to $C_b'-C_b' > C_b-C_b$ and $C_a'-C_m-C_{\phi 1} > C_a-C_m-C_{\phi 1}$ parameters to prevent unfavorable contacts between the phenyl rings that push the adjacent phenyl rings toward the unsubstituted pyrroles.[28] A similar trend was observed in the macrocycles of the cocrystallates examined in the present work with smaller difference in their values. For example, the difference in $C_b'-C_b' > C_b-C_b$ bond distance and $C_a'-C_m-C_{\phi 1} > C_a-C_m-C_{\phi 1}$ angles are lower in the cocrystals relative to parent porphyrins. Further, the elongation of $N\cdots N^i$ and contraction in $N'\cdots N'^i$ distances for M(TPP)$(Ph)_4 \cdot C_{60}$ cocrystals were observed in contrast to that of the corresponding M(TPP)$(Ph)_4$ structures.

As anticipated, their general trend in the core size of the cocrystals and parent M(TPP)(Ph)$_4$ structures follow the order:

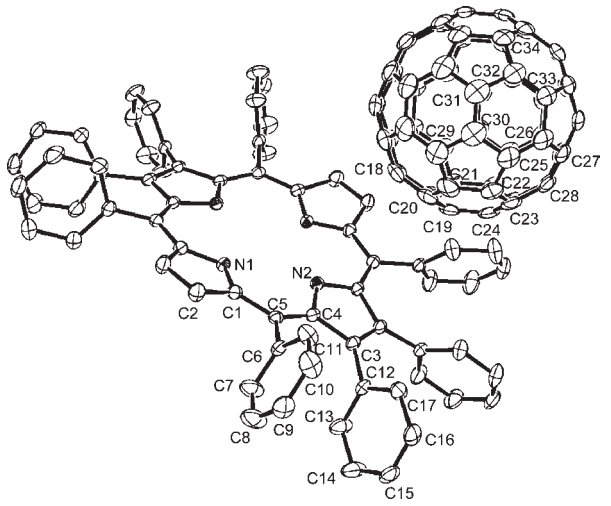

Figure 2. ORTEP of $H_2TPP(Ph)_4 \cdot C_{60}$ cocrystallate. The atoms of the asymmetric unit are labeled for clarity. Thermal ellipsoids at 40% probability level.

$H_2(TPP)(Ph)_4 > CuTPP(Ph)_4 > Co(TPP)(Ph)_4$ (Table 2). This suggests the contraction of the N_4 core by the core metal ion and redistribution of steric strain imposed by the close approach of C_{60} on the opposite faces of the porphyrin. Moreover, the average ($N\cdots N^{1}$ and $N'\cdots N'^{1}$) value in $H_2(TPP)(Ph)_4 \cdot C_{60}$ is marginally contracted when compared to $H_2(TPP)(Ph)_4$,[27a] and other M(TPP)(Ph)$_4 \cdot C_{60}$ (M = Co(II), Cu(II)) cocrystallates showed almost similar a core as in the corresponding M(TPP)(Ph)$_4$ structures (Table 2). The M−N′ is longer than the M−N bond distance in MTPP-(Ph)$_4$ and M(TPP)(Ph)$_4 \cdot C_{60}$ cocrystals; however, their mean bond distance is similar, but these are longer than the corresponding values in Co(TPP) (1.949(3) Å)[39] and Cu-(TPP) (1.981(7) Å).[40] The angle, $(N-M-N)_{adj}$, is 90°, and a decrease in the $(N-M-N)_{opp}$ angle from 180° in M(TPP)-(Ph)$_4 \cdot C_{60}$ (M = Co(II), Cu(II)) cocrystals (Table 2) suggests that the metal centers deviate from square planar geometry.[28b]

A comparison of geometrical parameters of the M(TPP)-(Ph)$_4 \cdot C_{60}$ cocrystals with the parent M(TPP)(Ph)$_4$ (M = 2H, Co(II), Cu(II)) structures indicates significant distortion of the macrocycles in the former cases (Table 2). In H_2(TPP)-(Ph)$_4 \cdot C_{60}$, the hydrogens are statistically disordered over all the four inner pyrrole nitrogens with slightly higher $C_a'-N'-C_a'$ than the C_a-N-C_a angle. The relative contraction

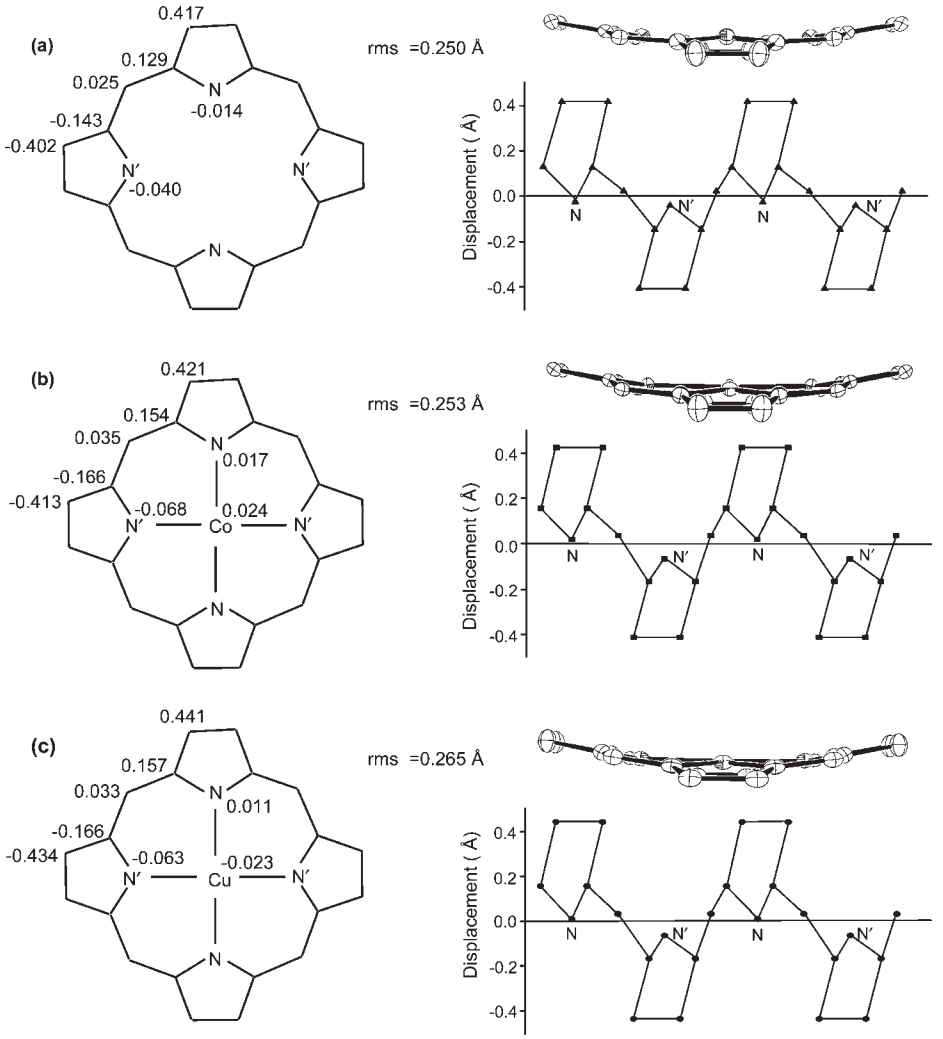

Figure 3. Left side shows mean plane deviation of the porphyrin ring core atoms, and right side is the side view of the macrocycle (phenyls are not shown for clarity) and linear deviation of the 24-atom core in (a) $H_2TPP(Ph)_4 \cdot C_{60}$, (b) $CoTPP(Ph)_4 \cdot C_{60}$, and (c) $CuTPP(Ph)_4 \cdot C_{60}$.

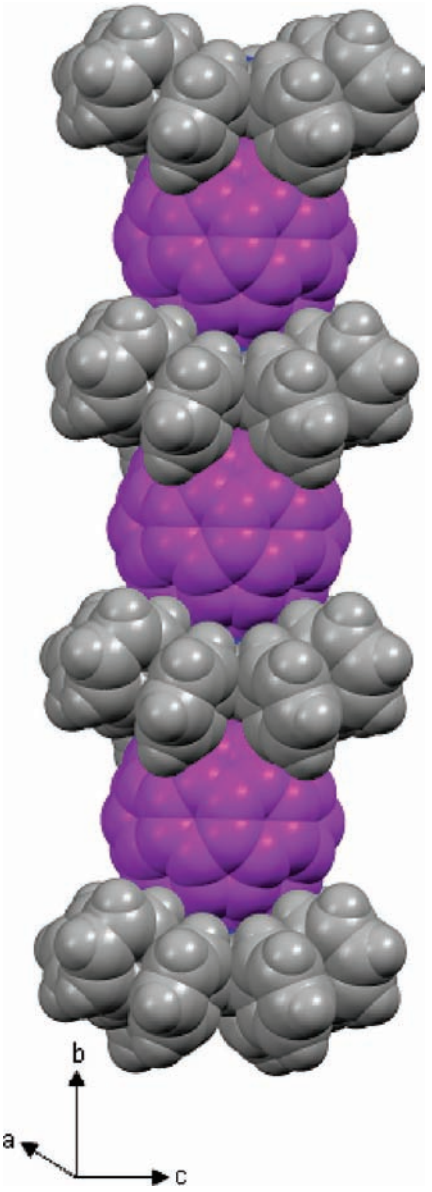

Figure 4. van der Waals packing diagram (100% vdw) of $H_2TPP(Ph)_4 \cdot C_{60}$ cocrystallate.

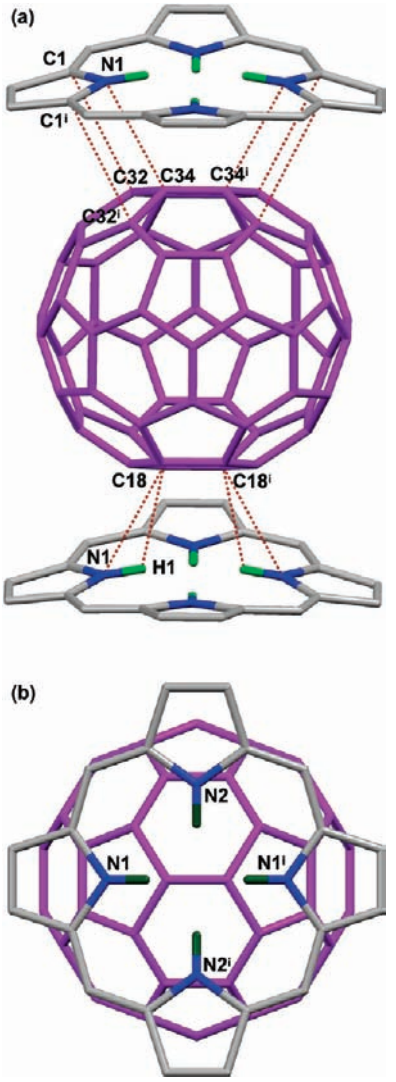

Figure 5. (a) Shows short intermolecular contacts between the porphyrin and C_{60} along the one-dimensional chains in $H_2TPP(Ph)_4 \cdot C_{60}$. (b) Relative orientation of C_{60} (shown in purple color) to the porphyrin ring. Short contact atoms are labeled for simplicity. The phenyl groups are not shown for clarity. Porphyrin: C, gray; N, blue; H, green. C_{60}, purple color.

and elongation of the core along the transannular direction is influenced by the core hydrogens to prevent bump into each other. Figure 3 shows the displacement of core atoms from the mean porphyrin ring plane, side view of the macrocyclic ring, and the linear displacement of the 24-atom core for the $M(TPP)(Ph)_4 \cdot C_{60}$ (M = 2H, Co(II), Cu(II)) cocrystallates. The comparison of the root-mean-square (rms) value which is the average deviation of the 24 atoms core from the least-squares plane is significantly higher in contrast to the parent porphyrins (Table 2). In addition, the *meso*-phenyl and β-pyrrole phenyl groups are oriented at angle of 66−74° with the $C_m-C_{\phi 1}$, and $C_b'-C_{\phi 2}$ bond distances are in the range 1.49−1.51 Å, indicating their conjugation with the porphyrin π-system is negligible. Table 2 shows there is a significant change in bond angles of the porphyrin ring in $H_2(TPP)(Ph)_4 \cdot C_{60}$ along the transannular substituted pyrrole direction versus the unsubstituted pyrrole direction which is induced by the $C_{60}-H_2(TPP)(Ph)_4$ intermolecular interactions; however, the angles are marginally affected in the case of $M(TPP)(Ph)_4 \cdot C_{60}$ (M = Co(II), Cu(II)) cocrystals. The nonplanarity of the porphyrin ring is reflected from an increase in torsional angles ($N'-C_a'-C_m-C_a$ and $C_b'-C_a'-C_m-C_{\phi 1}$) and a decrease in dihedral angles of the *meso*-phenyls in the cocrystallates compared to those of the corresponding parent porphyrins (Table 2). This shows the influence of convex C_{60} surface on the stereochemistry and conformational flexibility of these porphyrin macrocycles.

$M(TPP)(Ph)_4 \cdot C_{60}$ (M = 2H, Co(II), Cu(II)) cocrystallates exhibit similar packing motifs. The C_{60} molecules are positioned alternatively above and below the faces of the porphyrin to form a one-dimensional array. A representative one-dimensional array of $H_2(TPP)(Ph)_4 \cdot C_{60}$ is shown in Figure 4. The alternating face of the porphyrin has close contact with $C18-C18^i$ and $C34-C34^i$ bonds of C_{60} and are shorter in the $H_2(TPP)(Ph)_4 \cdot C_{60}$ complex (1.336(10)−1.352(9) Å) while they are elongated in $M(TPP)(Ph)_4 \cdot C_{60}$

(39) Madura, P.; Scheidt, W. R. *Inorg. Chem.* **1976**, *15*, 3182.
(40) Fleisher, E. B.; Miller, C. K.; Webb, L. E. *J. Am. Chem. Soc.* **1964**, *86*, 2342.

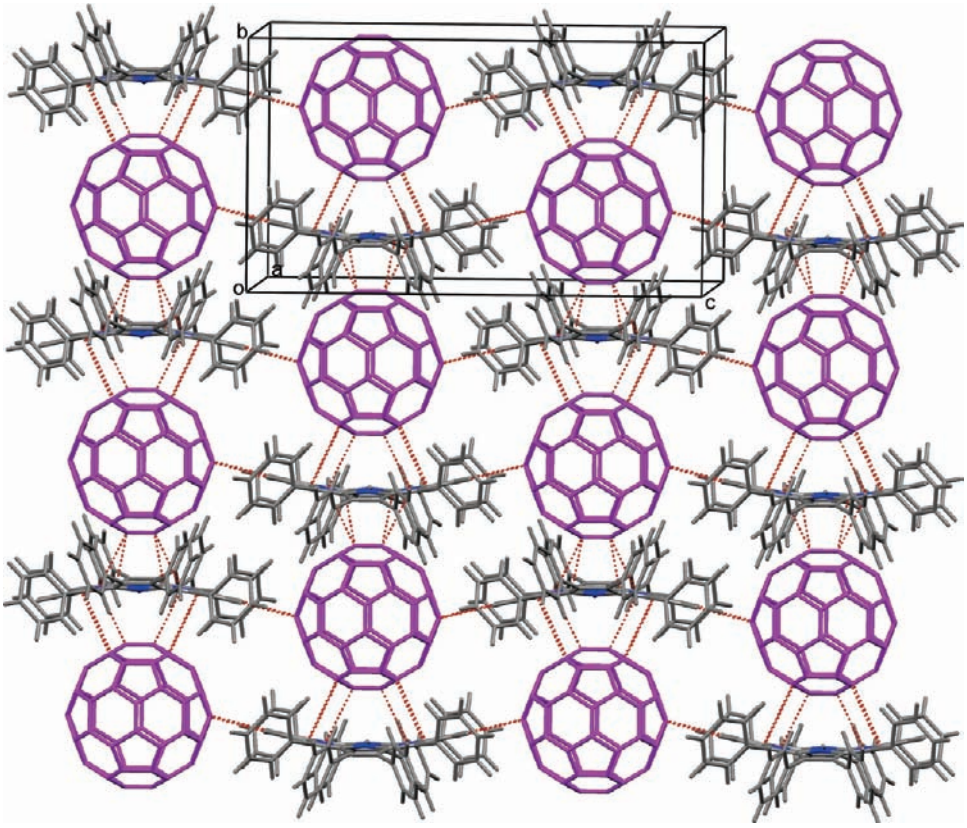

Figure 6. Packing motifs of $H_2TPP(Ph)_4 \cdot C_{60}$ showing the interconnected one-dimensional array via C−H···π interactions oriented parallel to unit cell side "*bc*" plane. Intermolecular contacts are shown in dotted red lines. Color scheme: porphyrin, C and H, gray; N, blue; C_{60}, purple.

(M = Co(II), Cu(II)) cocrystallates (1.357(15)−1.379(14) Å). Furthermore, the average C−C bond lengths of the 6:6 and 6:5 junctions in these cocrystals range from 1.34 to 1.39 Å and 1.44 to 1.48 Å, respectively. In the array, the centroid-to-centroid ($C_{60}\cdots C_{60}$) distance between the C_{60} molecules, which are in short contact with the porphyrin ring from its opposite faces, is 12.344 Å in $H_2(TPP(Ph)_4 \cdot C_{60}$, 12.266 Å in Co(TPP)-$(Ph)_4 \cdot C_{60}$, and 12.510 Å in $CuTPP(Ph)_4 \cdot C_{60}$ cocrystallates. The facial intermolecular contact on opposite faces of the porphyrin with the fullerene paracylene units is shown in Figure 5. It can be seen that the paracylene units are positioned in such a way that the 6:6 junction is aligned along the transannular unsubstituted pyrrole $N\cdots N^1$ direction. The short contact distance between the porphyrin−C_{60}, $N_{porphyrin}\cdots C(C_{60})$, is in the range 3.031(5)−3.056(5) Å while the shortest $C_{porphyrin}\cdots C_{60}$ is 3.329(3) Å. The separation between the mean porphyrin planes sandwiching the C_{60} in the array is 12.34 Å. These one-dimensional chains are interconnected via a very weak C−H···π (2.83 Å) between the porphyrin and C_{60} molecules to form an extended layerlike structure (Figure 6). The mean planes of the porphyrin ring from the adjacent array are offset with the vertical separation of 1.23 Å. These layers are interconnected via interporphyrin through a pair of phenyl−phenyl C−H···π (2.75 Å) interactions and are stacked perpendicular to the unit cell "*a*" axis to form an extended three-dimensional packing motif.

Similarly, $Co(TPP)(Ph)_4 \cdot C_{60}$ cocrystallate exhibited a one-dimensional array, and the C_{60} is sandwiched between the two porphyrin mean planes separated by 12.27 Å. The C_{60} molecules act as a bridge via a pair of weak C−H···$\pi(C_{60})$ (2.84 Å) contacts between the two adjacent one-dimensional

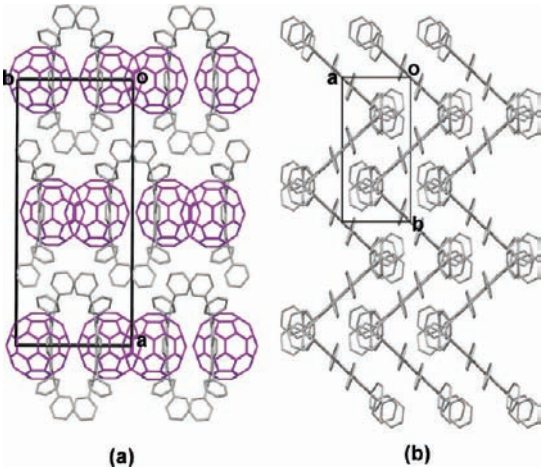

Figure 7. Molecular packing motifs of (a) $CuTPP(Ph)_4 \cdot C_{60}$ and (b) $CuTPP(Ph)_4$, complex view approximately down the "*c*" axis. Hydrogens are omitted for clarity. Color scheme: porphyrin, gray; and C_{60}, purple color.

arrays to form an extended layerlike structure. The closest vertical separation between the mean planes of the porphyrins from the adjacent array is 1.26 Å. The porphyrin face, with less C_{60} contacts in the array, features an additional four C−H···$\pi(C_{60})$ and phenyl−$C(C_{60})$ (2.89 Å) contacts. These extended layers are interconnected by weak interporphyrin C−H···π (2.77 Å) interactions and are stacked perpendicular to the unit cell "*a*" axis.

In $Cu(TPP)(Ph)_4 \cdot C_{60}$, C_{60} is sandwiched between the two porphyrin ring mean planes that are separated by 12.51 Å in

Table 3. Selected Mean Bond Lengths and Geometrical Parameters of the Macrocycle in $CuTPP(Ph)_4(CH_3)_4 \cdot C_{60}$, $Cu(TPP)(Ph)_4(CH_3)_4 \cdot CHCl_3$, and $CuTPP(Ph)_4$ Complexes

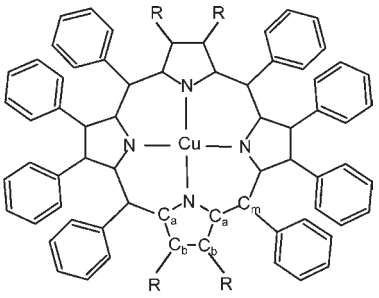

R = CH_3, $Cu(TPP)(Ph)_4(CH_3)_4 \cdot C_{60}$
R= CH_3, $Cu(TPP)(Ph)_4(CH_3)_4 \cdot CHCl_3$
R = H, $Cu(TPP)(Ph)_4$

	$Cu(TPP)(Ph)_4(CH_3)_4 \cdot C_{60}$	$Cu(TPP)(Ph)_4(CH_3)_4 \cdot CHCl_3$[a]	$Cu(TPP)(Ph)_4$
		Distance (Å)	
Cu−N	2.012(2)	1.946(2)	1.959(1)
Cu−N[b]	1.982(2)	1.962(2)	2.060(1)
N−C_a	1.379(3)	1.375(3)	1.383(2)
C_a−C_b	1.453(3)	1.453(4)	1.443(2)
C_b−C_b	1.361(3)	1.367(4)	1.354(2)
C_a−C_m	1.402(3)	1.407(4)	1.396(2)
		Angle (°)	
$(N-M-N)_{adj}$	90.2(1)	90.2(1)	90.0(6)
$(N-M-N)_{opp}$	173.8(1)	174.0(1)	180.0(1)
M−N−C_a	125.7(2)	124.8(2)	127.2(1)
N−C_a−C_m	123.5(2)	122.6(2)	125.8(2)
N−C_a−C_b	109.8(2)	109.0(2)	110.0(2)
C_a−N−C_a	106.2(2)	107.6(2)	105.7(2)
C_b−C_a−C_m	126.3(2)	127.9(2)	124.3(2)
C_a−C_m−C_a	124.0(2)	122.1(2)	124.2(2)
		Geometrical Parameters (Å)	
rms	0.236(2)	0.391(2)	0.012(2)
N···N[i]	4.016	3.885	3.918
(N···N[i])[c]	3.959	3.919	4.120
		Dihedral Angle (°)	
meso-phenyl	69.6(1)	54.0(1)	74.1(1)
β-phenyl	68.0(1)	66.3(1)	71.3(1)
pyrrole	15.0(1)	21.5(6)	0.6(1)

[a] Data from ref 32a. [b] Distance for *β*-phenyl substituted pyrrole. [c] Along *β*-phenyl substituted pyrrole direction.

the array. These one-dimensional chains are interconnected by pair of $(C-H)_{porphyrin}\cdots\pi(C_{60})$ (2.84 Å) contacts to induce a layerlike structure (*bc* plane), similar to the $H_2TPP(Ph)_4 \cdot C_{60}$ structure. The closest porphyrin mean planes in the neighboring one-dimensional array are offset with a vertical separation of 1.34 Å. The weakly held layers are connected through weak interporphyrin C−H···*π* (2.76 Å) contacts, and the layers stack perpendicular to unit cell "*a*" axis. Interestingly, in the cocrystallates, the *β*-phenyl groups are bent toward one face of the porphyrin showing less contact with the C_{60} while the *meso*-phenyls are almost in one plane. This is further evidenced from the increase (11−14°) in $C_m-C_a'-C_b'-C_{\phi 2}$ torsional angles, when compared to those angles in $M(TPP)(Ph)_4$ structures (1 to 2°).

A comparison of $Cu(TPP)(Ph)_4$ with $Cu(TPP)(Ph)_4 \cdot C_{60}$ shows considerable change in molecular packing, indicating structural variation induced by the incorporation of C_{60} into the porphyrin lattice. Molecular packing motifs for $Cu(TPP)(Ph)_4 \cdot C_{60}$ complex oriented along the unit cell "*c*" axis is shown in Figure 7a. Porphyrin and C_{60} molecules stack alternately front and back along the unit cell "*c*" axis in the $CuTPP(Ph)_4 \cdot C_{60}$. The view is perpendicular to a one-dimensional array and they slip stack along the unit cell "*c*" axis. The packing motif of the $Cu(TPP)(Ph)_4$ structure is shown along the unit cell "*c*" axis (Figure 7b). The one-dimensional slip-stacked porphyrin chains are oriented approximately along the unit cell "*a*" axis and are interconnected through a pair of symmetry related weak C−H···*π* (2.77−2.87 Å) interactions on each face of the porphyrin. Each array is bridged by two symmetry related interporphyrin weak C−H···*π* (2.84−2.87 Å) contacts. The porphyrins from the adjacent array are oriented in a zigzag fashion as shown in Figure 7b. The molecules are largely held in the lattice by weak C−H···*π* and van der Waals interactions. A similar packing motif was observed in $Co(TPP)(Ph)_4 \cdot C_{60}$ and $Co(TPP)(Ph)_4$ structures.

To determine the effect of the nonplanar porphyrin ring *π*-system on the convex fullerene surface, we examined the

structure of Cu(TPP)$(Ph)_4(CH_3)_4\cdot C_{60}$ cocrystal. It crystallized in a monoclinic space group $C2/c$ with $Z = 4$. The asymmetric unit has one-half of each porphyrin and C_{60}, and both have a 2-fold rotational axis parallel to unit cell "*b*". The selected mean bond lengths and angles of the 24-atom core are listed in Table 3. For comparison, the data of Cu(TPP)-$(Ph)_4(CH_3)_4\cdot CHCl_3$[32a] and Cu(TPP)$(Ph)_4$ structures are also listed in Table 3. The mean C−C bond distances of the 6:6 and 6:5 junctions of the C_{60} unit in Cu(TPP)$(Ph)_4(CH_3)_4\cdot C_{60}$ has the range from 1.33 to 1.39 Å and 1.44 to 1.47 Å, respectively. Interestingly, the Cu−N bond distance in Cu-(TPP)$(Ph)_4(CH_3)_4\cdot C_{60}$ cocrystallate is longer than the $Cu-N^b$ distance, and it is perhaps due to steric crowding of the peripheral substituents and/or porphyrin$\cdots C_{60}$ interactions. Moreover, the average M−N bond distance (1.997(2) Å) in the cocrystallate is longer than that reported for Cu(TPP)$(Ph)_4(CH_3)_4\cdot CHCl_3$ (1.954(2) Å)[32a] and shorter than Cu(TPP)$(Ph)_4\cdot C_2H_2Cl_4$ (2.010(1) Å).[32b] This is also reflected from an increase in $N\cdots N^i$ and decrease in $(N\cdots N^i)^e$ distances in Cu(TPP)$(Ph)_4(CH_3)_4\cdot C_{60}$ and reveal the contraction of the core along the antipodal pyrroles with methyl groups compared to the other transannular pyrroles with phenyl groups, and an opposite trend is reported for the Cu(TPP)$(Ph)_4(CH_3)_4\cdot CHCl_3$ structure.[32a] The mean ($N\cdots N$ and $(N\cdots N)^e$) separation of the macrocycle in these structures varies in the order Cu(TPP)$(Ph)_4(CH_3)_4\cdot CHCl_3$ (3.90 Å) < Cu(TPP)$(Ph)_4(CH_3)_4\cdot C_{60}$ (3.99 Å) < Cu(TPP)-$(Ph)_4$ (4.02 Å). The bond lengths of the macrocycle of the cocrystallates are comparable with the macrocyclic ring in Cu(TPP)$(Ph)_4(CH_3)_4\cdot CHCl_3$ and Cu(TPP)$(Ph)_4$ complexes. In addition, the geometry around the Cu(II) centers shows distorted square planar geometry in contrast to that observed in the Cu(TPP)$(Ph)_4$ structure (Table 3). The comparison of core bond angles of the porphyrin ring in Cu(TPP)$(Ph)_4$-$(CH_3)_4\cdot C_{60}$ and Cu(TPP)$(Ph)_4(CH_3)_4\cdot CHCl_3$ structures revealed an increase in $C_b-C_a-C_m$ angle and considerable decrease in $M-N-C_a$ and $N-C_a-C_m$ angles when compared to planar Cu(TPP)$(Ph)_4$. The extent of variation in these angles indicates the decreased nonplanarity of the macrocyclic ring in Cu(TPP)$(Ph)_4(CH_3)_4\cdot C_{60}$ relative to Cu(TPP)$(Ph)_4(CH_3)_4\cdot CHCl_3$. This is further evidenced from their rms values, the dihedral angles for the *meso*-phenyl, and β-phenyl and pyrrole groups relative to porphyrin ring mean plane (Table 3).

The molecular packing motif of Cu(TPP)$(Ph)_4(CH_3)_4\cdot C_{60}$ cocrystal is quite comparable to M(TPP)$(Ph)_4\cdot C_{60}$ cocrystals. The porphyrin and C_{60} molecules are arranged alternatively along the unit cell "*b*" axis to form a one-dimensional array. Figure 8 shows the interaction between the porphyrins and the fullerene along the one-dimensional chain. Along the column, the C_{60} is sandwiched between the porphyrin mean planes separated by 12.89 Å. On one face of the porphyrin, the β-phenyl groups bent toward the C_{60} with short contact distances between porphyrin (*o*-phenyl hydrogen)$\cdots C(C_{60})$ C−H$\cdots\pi$ (2.81−2.86 Å), and $(C_{60})C\cdots C_{porphyrin}$, $\pi\cdots\pi$ (3.179(5)−3.250(7) Å) interactions were observed. The other opposite face of the porphyrin is dominated by a core Cu(II) ion interacting with the $C55-C55^i$ double bond 6:6 junction with the short $C_{C60}\cdots$Cu contacts. Figure 8b shows the relative orientation of the paracylene unit of the C_{60} to the Cu(TPP)-$(Ph)_4(CH_3)_4$ macrocyclic ring. In the case of Cu(TPP)$(Ph)_4$-$(CH_3)_4\cdot C_{60}$ complex, the 6:6 junction is oriented at an angle

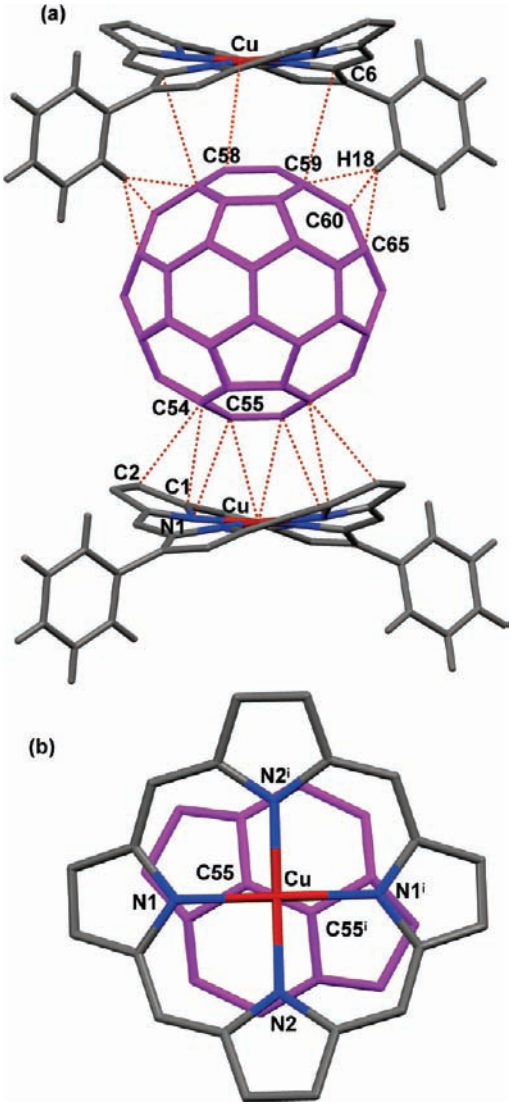

Figure 8. (a) Shows porphyrin−fullerene close contacts along the one-dimensional chain of CuTPP$(Ph)_4(CH_3)_4\cdot C_{60}$ complex. The short contact atoms are labeled for clarity. (b) Feature relative orientation of the paracylene unit of C_{60} relative to the porphyrin ring. Porphyrin: C and H, gray; N, blue; and Cu, red. C_{60}, purple color.

of 25.6° relative to the $(N1-Cu-N1^i)_{opp}$ angle while it is parallel to that angle in MTPP$(Ph)_4\cdot C_{60}$ (M = Co(II), Cu(II)) cocrystallates. In these cocrystallates, the *meso*-phenyl and β-pyrrole phenyl groups are approximately bent in opposite faces to the porphyrin mean plane. The closest vertical distance between the offset porphyrin mean planes in the adjacent column is 3.00 Å, and they are connected via porphyrin$\cdots C(C_{60})$ and C−H$\cdots\pi$ (2.77 Å) contacts resulting in layerlike structure (Figure 9). These layers interact with the adjacent layer via interporphyrin, C−H$\cdots\pi$ (2.68 Å), interactions to form three-dimensional packing. The $C_{60}\cdots C_{60}$ interaction between the adjacent columns shows the closest C$\cdots$C contact distance is greater than 5.4 Å, indicating negligible inter-C_{60} interactions along the layer or between the layers. A comparison of the packing along the unit cell *c*-axis of Cu(TPP)$(Ph)_4(CH_3)_4\cdot C_{60}$ with Cu(TPP)$(Ph)_4(CH_3)_4\cdot$ $CHCl_3$ showed that the C_{60} replaces the $CHCl_3$ between the porphyrin faces.

In M(TPP)$(Ph)_4\cdot C_{60}$ and M(TPP)$(Ph)_4(CH_3)_4\cdot C_{60}$ cocrystallates, the observed porphyrin−C_{60} short contact

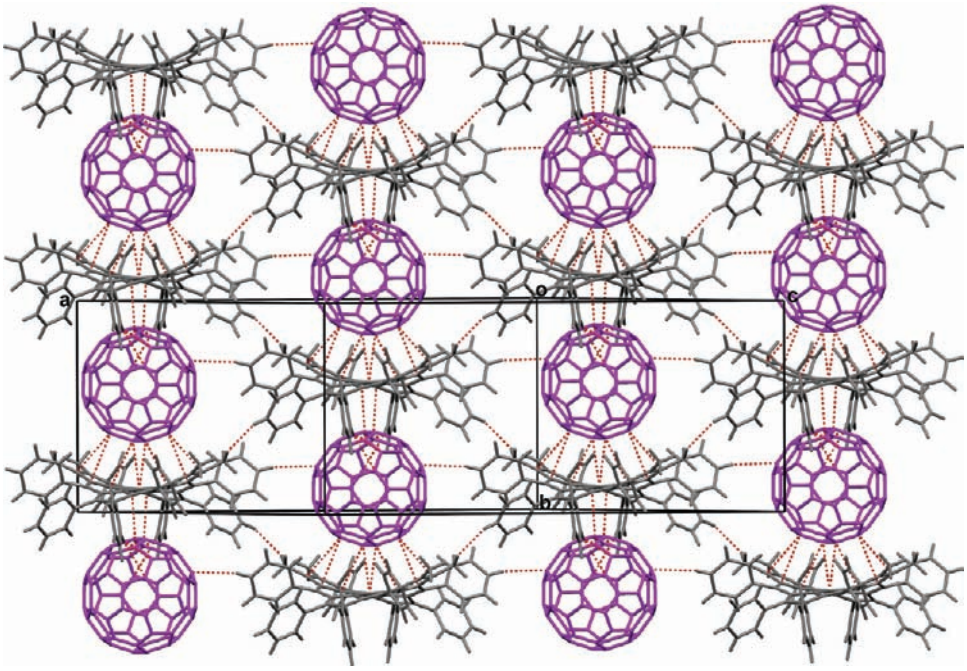

Figure 9. Molecular packing motifs of $CuTPP(Ph)_4(CH_3)_4 \cdot C_{60}$ complex showing the interconnected one-dimensional array oriented parallel to unit cell "*ab*" plane. Intermolecular contacts are shown in dotted red lines. Porphyrin: C and H, gray; N, blue; Cu, red. C_{60}, purple color.

distances are comparable to the reported cocrystallates.[13,14] The closest contact between the porphyrin−C_{60} is dominated by $N_{porphyrin} \cdots C(C_{60})$ (2.923(7)−3.164(4) Å), $C_{porphyrin} \cdots C(C_{60})$ (3.179(5)−3.329(3) Å), and $M \cdots C_{60}$ (2.761(6)−3.627(5) Å) interactions. The $C_{porphyrin} \cdots C(C_{60})$ and $(C_{60})C \cdots N_{porphyrin}$ short contact distances in $H_2(TPP)(Ph)_4 \cdot C_{60}$ (3.329 Å and 3.031(5) Å) are comparable to 3.37 Å and 3.02−3.12 Å of $H_2TPP \cdot C_{60} \cdot (C_7H_8)_3$ and 3.41−3.70 Å and 2.96 Å of $H_2TPP(C_{60})_2 \cdot (C_6H_6)_n$ (n = 3, 4) cocrystallates.[14b] Similarly, the $N_{porphyrin} \cdots C(C_{60})$ close contact distances in the range 3.02−3.12 Å were reported for $H_2TPP \cdot C_{60}(C_7H_8)_3$ cocrystallate.[14a] The longer $Co \cdots C(C_{60})$ distance indicates the oxidation state of the cobalt center is divalent since the reported distance was in the range of 2.67−2.78 Å for both $Co(TPP) \cdot C_{60}(C_6H_4Cl_2)_{2.5}$[14d] and $Co(OEP) \cdot C_{60} \cdot CHCl_3$[13a] cocrystallates. The $Co \cdots C(C_{60})$ contact distances in the saddle-shaped porphyrin ring of $Co(T(4'\text{-}OCH_3\ Ph)P) \cdot C_{60}$ cocrystallate[14c] was 3.16−3.21 Å while a planar macrocycle containing $Co(T(4'\text{-}OCH_3\ Ph)P) \cdot (C_{60})_2 \cdot 3(toluene)$ showed shorter distances (2.64−3.55 Å).[14c] The crystal structure of the covalently bonded CoTPP−C_{60} diad showed close contact distances of 2.726 Å and 2.713 Å for $Co \cdots C_{C60}$, and such interactions were suggested to be weak σ-donor ($(C_{60})C \rightarrow Co(CoTPP)$) and π-acceptor (porphyrin $\rightarrow \pi(C_{60})$) interactions.[21f] Much shorter $Co \cdots C(C_{60})$ contacts 2.28−2.32 Å were indicative of a $Co-C(C_{60})$ covalent bond in the $Co(TPP) \cdot (C_{60})^-$ system.[14d] The density functional theoretical calculations on metalloporphine−C_{60}, $MP \cdot C_{60}$ (M = Co(II), Ni(II), Cu(II), and Zn(II)), complexes indicated shorter $Co \cdots C(C_{60})$ close contact distances than other $M \cdots C(C_{60})$ contacts.[16c]

The observed value of the shortest $Cu \cdots C(C_{60})$ distances in $Cu(TPP)(Ph)_4 \cdot C_{60}$ is 2.889(4) Å and for $Cu(TPP)(Ph)_4(CH_3)_4 \cdot C_{60}$ is 3.036(3) Å when compared to those reported in nonplanar $[Cu(TPP)]_2 \cdot C_{60}$ (3.47 Å)[14b] and $Cu(OEP) \cdot C_{60}(CHCl_3)_2$ (3.02 Å)[13a] crystallates. The majority of the reported porphyrin−C_{60} cocrystals showed near planarity of the porphyrin ring. The $M(TPP)(Ph)_4 \cdot C_{60}$ cocrystals indicate a nonplanar macrocycle (rms = 0.265 Å) which is comparable to that reported for a $(Cu(TPP))_2 \cdot C_{60}$ structure (rms = 0.263 Å). The use of a nonplanar porphyrin ring as in $Cu(TPP)(Ph)_4(CH_3)_4 \cdot C_{60}$ revealed interesting structural features that the nonplanarity of the macrocycle decreases relative to that of the $Cu(TPP)(Ph)_4(CH_3)_4 \cdot CHCl_3$ structure.[32] The dense close packing of spherical C_{60} with the flat-disk like porphyrins is rather less favorable. The conformational flexibility of the planar macrocycle in $M(TPP)(Ph)_4$ derivatives acquire the nonplanar conformation to induce $porphyrin \cdots C_{60}$ interactions and perhaps provide effective close packing in these structures. For all the structures examined in this study, the short contact distances are less than the sum of their van der Waals radii,[41] indicating the weak intermolecular interactions.[42]

The porphyrin rings in $M(TPP)(Ph)_4 \cdot C_{60}$ and $M(TPP)(Ph)_4(CH_3)_4 \cdot C_{60}$ cocrystallates were examined by normal-coordinate structure decomposition (NSD) analysis.[43] The out-of-plane displacement (D_{oop}) and in-plane displacement (D_{ip}) values from the minimum basis set of core atoms of the macrocyclic ring in the various cocrystallates and their corresponding parent porphyrins are also listed in Table 4. The sum of all the displacements and their percentage distortions were calculated by neglecting the sign on the values. It is evident from the D_{oop} values that the $M(TPP)(Ph)_4 \cdot C_{60}$ cocrystallates feature enhanced nonplanar

(41) Bondi, A. *J. Phys. Chem.* **1964**, *68*, 441.
(42) (a) Desiraju, G. R. *Acc. Chem. Res.* **2002**, *35*, 565. (b) Desiraju, G. R.; Steiner, T. *The weak hydrogen bond in structural chemistry and biology*; IUCr Monographs on Crystallography 9; Oxford University Press: Oxford, 1999, pp 215.
(43) (a) Jentzen, W.; Ma, J.-M.; Shelnutt, J. A. *Biophys. J.* **1998**, *74*, 753. (b) Sun, L.; Jentzen, W.; Shelnutt, J. A. The Normal Coordinate Structural Decomposition Engine. http://jasheln.unm.edu/jasheln/content/nsd/NSDengine.

Table 4. Normal-Coordinate Structure Decomposition Analysis of Macrocycles in Porphyrin−C_{60} Cocrystallates and Their Parent Porphyrins[a]

Out of Plane Displacements (Å)

	D_{oop}	B_{2u}, *sad*	B_{1u}, *ruf*	A_{2u}, *dom*	E_g(x), *wav*(*x*)	E_g(y), *wav*(*y*)	A_{1u}, *prop*	sum	*sad*/sum (%)	*ruf*/sum (%)	*dom*/sum (%)
1	1.2075	1.2064	0.0000	−0.0510	0.0000	0.0000	0.0000	1.2574	95.9	0	4.0
2	1.2616	−1.2609	0.0000	0.0422	0.0000	0.0000	0.0000	1.3031	96.8	0	3.2
3	1.3152	−1.3145	0.0000	0.0420	0.0000	0.0000	0.0000	1.3565	96.9	0	3.1
4[b]	0.0350	−0.0002	0.0000	−0.0001	−0.0346	0.0052	−0.0001	0.0402	0.5	0	0.25
5[c]	0.0261	0.0000	−0.0002	−0.0000	−0.0144	0.0218	0.0000	0.0364	0	0.55	0
6[c]	0.0327	−0.0001	−0.0001	0.0003	−0.0247	−0.0214	0.0002	0.0468	0.21	0.21	0.64
7	2.5678	−2.5417	0.2414	0.2733	0.0000	0.0000	−0.0170	3.0734	82.7	7.85	8.9
8	3.2119	−2.7295	1.6893	0.0898	0.0000	0.0000	0.0667	4.5753	59.7	36.9	2.0

In-Plane Displacements (Å)

	D_{ip}	B_{2g}(*m-str*)	B_{1g}(*N-str*)	E_u(x) (*trn*)	E_u(y) (*trn*)	A_{1g}(*bre*)	A_{2g}(*rot*)	sum	B_{2g}/sum (%)	B_{1g}/sum (%)	A_{1g}/sum (%)
1	0.2526	0.0000	−0.1997	0.0006	−0.0007	0.1547	0.0000	0.3557	0	56.1	43.5
2	0.1532	0.0000	−0.1179	0.0000	0.0003	−0.0979	0.0000	0.2161	0	54.5	45.3
3	0.1449	0.0000	−0.1422	0.0008	0.0000	−0.0277	0.0000	0.1707	0	83.3	16.2
4	0.4412	−0.0231	0.3643	0.0002	0.0002	0.2477	0.0053	0.6408	3.6	56.8	38.6
5	0.1840	−0.0063	−0.1819	−0.0001	0.0001	0.0257	0.0081	0.2222	2.8	81.8	11.5
6	0.2555	−0.0063	−0.2360	0.0000	−0.0001	0.0969	0.0112	0.3505	1.8	67.3	27.6
7	0.3012	−0.0035	−0.0697	0.0001	0.0001	−0.2928	−0.0119	0.3781	0.9	18.4	77.4
8	0.6814	−0.0386	−0.0132	0.0004	−0.0003	−0.6788	−0.0428	0.7741	5.0	1.7	87.7

[a] **1**, H_2(TPP)(Ph)$_4$·C_{60}; **2**, Co(TPP)(Ph)$_4$·C_{60}; **3**, Cu(TPP)(Ph)$_4$·C_{60}; **4**, H_2(TPP)(Ph)$_4$; **5**, Co(TPP)(Ph)$_4$; **6**, Cu(TPP)(Ph)$_4$; **7**, Cu(TPP)(Ph)$_4$(CH$_3$)$_4$·C_{60}; **8**, Cu(TPP)(Ph)$_4$(CH$_3$)$_4$·$CHCl_3$. [b] Mainly wave $E_g(x)$ distortion. [c] Combination of wave ($E_g(x)$ and $E_g(y)$) distortions.

distortion of the macrocyclic ring in contrast to that observed for parent M(TPP)(Ph)$_4$ structures. The magnitude of distortion observed in these cocrystallates is predominantly from *sad* (B_{2u}) combined with minor *dom* (A_{2u}) distortions. D_{oop} of the core atoms in M(TPP)(Ph)$_4$ (M = 2H, Co(II), Cu(II)) derivatives showed negligible distortion of the porphyrin ring with major contribution from the wave [$E_g(x)$, $E_g(y)$] distortions. Similarly, the in-plane displacement of the core atoms in M(TPP)(Ph)$_4$·C_{60} cocrystallates showed mainly contributions from *N-str* (B_{1g}) and ring *bre* (A_{1g}) distortions. M(TPP)(Ph)$_4$ (M = 2H, Co(II), Cu(II)) structures revealed a higher D_{ip} value relative to the corresponding M(TPP)(Ph)$_4$·C_{60} structures. Further, H_2(TPP)(Ph)$_4$·C_{60} has higher contribution from *N-str* and is decrement in *bre* when compared to that observed in M(TPP)(Ph)$_4$·C_{60} (M = Co(II), Cu(II)) cocrystallates. However, macrocycles in these systems showed lower in-plane displacements in contrast to the corresponding parent porphyrins.

The Cu(TPP)(Ph)$_4$(CH$_3$)$_4$·C_{60} complex[31] exhibited a lower D_{oop} value, indicating decreased nonplanarity of the porphyrin ring when compared to that of the Cu(TPP)(Ph)$_4$(CH$_3$)$_4$·$CHCl_3$ complex (Table 4). The D_{oop} is composed of major *sad,* minor *ruf* and *dom* distortions. However, the parent Cu(TPP)(Ph)$_4$(CH$_3$)$_4$·$CHCl_3$ complex showed higher nonplanarity with major contribution from mainly *sad*, minor *ruf* and *prop* distortions. The Cu(TPP)(Ph)$_4$(CH$_3$)$_4$·$CHCl_3$ complex features predominantly *bre* with gentle *m-str* and *rot* distortions while Cu(TPP)(Ph)$_4$(CH$_3$)$_4$·C_{60} has predominantly *bre* and minor *N-str* distortions for in-plane displacements of their 24-atoms core. The cocrystallates show enhanced distortion of the macrocyclic ring in M(TPP)(Ph)$_4$·C_{60} while a decrement in distortion is observed for nonplanar macrocycle containing M(TPP)(Ph)$_4$(CH$_3$)$_4$·C_{60} cocrystallate. This suggests the influence of a convex fullerene surface on the stereochemistry of the planar porphyrin macrocycle in these cocrystallates.

Conclusions

Crystal structures of a new series of substituted porphyrin−C_{60} cocrystallates were examined to elucidate the role of C_{60} on the stereochemistry of the porphyrin host. All the cocrystallates of porphyrin−C_{60} indicate 1:1 stoichiometry and are free of lattice solvates. The short metal−C_{60} intermolecular contacts in M(TPP)(Ph)$_4$·C_{60} (M = Co(II), Cu(II)) cocrystals suggest greater fullerene porphyrin interactions than that observed for the H_2TPP(Ph)$_4$·C_{60} structure. The macrocyclic rings in these cocrystallates are nonplanar (rms < 0.27 Å) while the parent porphyrin rings have more planar geometry (rms < 0.016 Å). The use of nonplanar host in the Cu(TPP)(Ph)$_4$(CH$_3$)$_4$·C_{60} cocrystal revealed decreased nonplanarity of the porphyrin ring in contrast to that found in the Cu(TPP)(Ph)$_4$(CH$_3$)$_4$·$CHCl_3$ structure. Molecular packing diagrams of these cocrystallates indicate essentially a one-dimensional array induced by weak porphyrin−C_{60} contacts, and these chains are held by weak C−H···π and van der Waals interactions. The induced nonplanarity in these structures suggests the conformational flexibility that allows octaphenylporphyrin derivatives to adopt complementary surface to the convex C_{60}. Normal-coordinate structure decomposition analysis for the out-of-plane displacement (D_{oop}) with minimal basis set in the cocystallates (M(TPP)(Ph)$_4$·C_{60}) revealed predominantly *saddled* and gentle *domed* distortions, while the parent M(TPP)(Ph)$_4$ structures indicated very minimal *wave* distortions. The nonplanar porphyrin containing cocrystal, Cu(TPP)(Ph)$_4$(CH$_3$)$_4$·C_{60}, shows largely *saddle* combined with minimal *ruffled* and *domed* distortions relative to *saddle* combined with enhanced *ruffled* and negligible *domed* distortions observed for the parent Cu(TPP)(Ph)$_4$(CH$_3$)$_4$·$CHCl_3$ structure. The nonplanar geometry of the porphyrin ring in the M(TPP)(Ph)$_4$·C_{60} cocrystallates is perhaps due to porphyrin−C_{60} intermolecular interactions, and crystal packing forces cannot be neglected in these systems.

Acknowledgment. This research work was supported by a research grant from Department of Science and Technology, Government of India to P.B. We thank Dr. Varghese (SAIF, IIT Madras) for helpful discussion, Mr. V. Ramkumar for X-ray data collection, and Department of Chemistry at IIT Madras for single crystal X-rd facility.

Note Added after ASAP Publication. This paper was published on the Web on August 19, 2010. Additional text was added to the first sentence of the Abstract and the corrected version was reposted on September 13, 2010.

Supporting Information Available: Includes ORTEPs, intermolecular contacts, van der Waals packing diagrams, mean plane deviation diagrams of the porphyrin ring in $M(TPP)(Ph)_4 \cdot C_{60}$ cocrystallates and $M(TPP)(Ph)_4$ (M = Co(II), Cu(II)) complexes. Crystallographic information file (CIF) format for all six structures is available. This material is available free of charge via the Internet at http://pubs.acs.org.